

Experimental study on the evading behaviour of single pedestrians encountering an obstacle

Xiaolu Jia¹, Claudio Feliciani², Daichi Yanagisawa^{2,3}, Katsuhiro Nishinari^{2,3}

¹ Department of Advanced Interdisciplinary Studies, School of Engineering, The University of Tokyo
4-6-1 Komaba, Meguro-ku, Tokyo 153-8904 Japan
xiaolujia@g.ecc.u-tokyo.ac.jp

² Research Center for Advanced Science and Technology, The University of Tokyo
4-6-1 Komaba, Meguro-ku, Tokyo 153-8904 Japan
feliciani@jamology.rcast.u-tokyo.ac.jp

³ Department of Aeronautics and Astronautics, Graduate School of Engineering, The University of Tokyo
7-3-1 Hongo, Bunkyo-ku, Tokyo 113-8656, Japan
tDaichi@mail.ecc.u-tokyo.ac.jp; tknishi@mail.ecc.u-tokyo.ac.jp

Abstract –Present simulation and experimental research still have deficiency in depicting the evading behaviour of single pedestrians confronting with an obstacle, which is the basis for the study of crowd dynamics affected by obstacles in real life. Therefore, this study will conduct experiments with a bar-shaped obstacle in the middle of a corridor and explore the corresponding general and particular features of single pedestrians. Particularly, the variation of pedestrian velocity and trajectory under different-sized obstacles will be illustrated. By taking the average velocity and trajectories of the 32 participants, it could be concluded that pedestrians would walk at a velocity of about 1.5 m/s without being affected by the size of obstacle. Besides, pedestrians tend to pass a location about 0.4 meters away from the obstacle edge that is perpendicular to walking direction. Furthermore, pedestrians tend to begin and finish evading the obstacle at locations respectively about 4.40 meters and 4.85 meters away from the obstacle. We also found a heterogeneity in the evading behaviour and pedestrians could be classified into four types accordingly. Results of this study are expected to provide reliable evidence for agent-based modelling in the future.

Keywords: evading behaviour; obstacle size; velocity variation; evading trajectory; individual experiments

1. Introduction

Most walking facilities, such as sports venues, traffic terminals, and residential complexes, are composed of obstacles including walls, pillars, and fences for pedestrian traffic. Understanding the way in which obstacles affect pedestrian behaviour is essential to the optimization of architectural layouts and pedestrian organization schemes for better evacuation efficiency, comfort, and security. Bar-shaped obstacles such as walls, in particular, are practical for better pedestrian traffic management because they can be used either as architectural boundaries or as obstacles to fulfil certain service functions. In this study, we will explore the influence of bar-shaped obstacle on pedestrian behaviour.

The effects of obstacles on the evacuation behaviour of crowded pedestrians are often simulated by agent-based modelling, which could reproduce mass behaviour through setting certain movement rules to single agent. The most widely applicable microscopic simulation models include the cellular automata (CA) model [1], social force model (SFM) [2] and velocity obstacle method (VO) [3,4,5] in the state-of-the-art research. The CA model divides the space into discrete grids and its agents could only choose to move to the neighbouring grids or stay still, which greatly decreases calculation burden through limiting the moveable direction and velocity of pedestrians. In SFM, pedestrians are regarded as particles driven by psychological and physical forces from obstacles or other pedestrians, so they could enjoy more freedom in choosing walking direction and velocity. In VO model, the collision-avoidance behaviour of pedestrians is also affected by relative velocity except for relative location, and pedestrians could choose optimal collision-free velocity when confronting with obstacles.

The three types of models could reproduce interesting phenomena. For instance, some studies showed that placing a circle-shaped or bar-shaped obstacle at certain distance away from the exit could help improve flow rate [6] or decrease evacuation time [7]. However, these models are not necessarily able to reproduce the real evading behaviour of single pedestrian before an obstacle. To be specific, although some simulation models could emulate individual pedestrians evading obstacles [8,9] and even reproduce varied evading behaviours controlled with parameters [10], experimental evidence to validate the simulations remains insufficient.

Therefore, many scholars have conducted experiments that could help verify whether the modelling rules were in accordance with real pedestrian evading behaviour. Some studies set a static pedestrian as the obstacle in the middle of the corridor and numerically depicted the features of evading behaviour [11,12]. The distance between the centroids of individual pedestrian and the obstacle when the pedestrian began to change his movement direction ranged from 0.5 m to 4.25 m in [11] and from 1.5 m to 4 m in [12]. However, pedestrian behaviour may change when confronting real obstacles instead of static pedestrian, making the experimental results difficult to apply when bar-shaped obstacles are present.

Moreover, the existing experimental analyses of evading behaviour are not adequate. Most studies only depicted pedestrian trajectories and provided an average velocity of single pedestrians without an in-depth analysis on the effect of obstacle size on the heterogeneity of pedestrian evading behaviour. Therefore, through conducting experiments using real obstacle, this study will explore the common and particular features of the evading behaviour of different pedestrians and illustrate the influence of obstacle size variation on evading behaviour.

2. Experimental setup

Experiments have been conducted to investigate the way in which the size of bar-shaped obstacles will affect the evading behaviour of single pedestrians. The experiments were held on November 4th, 2017 in the Lecture Hall of RCAST Building 4, the University of Tokyo, Japan. 32 male students, whose ages ranged from 20 to 24, have participated in the experiments.

A camera was set above the horizontal axis of the corridor and fixed at 6 meters above the ground. Recording of the camera was adjusted to full HD mode (1920×1080 pixel) with a frame rate of 30 fps. With the videos of the experiments as raw data, the recognition and tracking of pedestrian locations under each frame could be achieved by using PeTrack software (version 0.8) [13], and the variations of velocity and trajectory in different scenarios could be obtained accordingly.

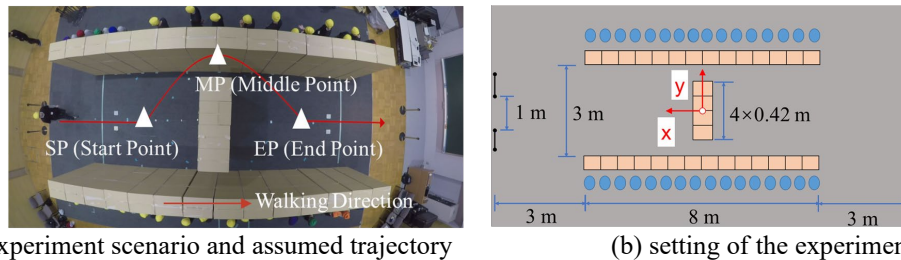


Fig. 1: Experimental scenario with a bar-shaped obstacle formed from four cardboard boxes ($box=4$) in the middle of the corridor. The width, depth, and height of each box is 0.42, 0.46, and 2.1 meters respectively.

As shown in Fig. 1(a), we constructed the walls of a corridor and an obstacle in the middle of the corridor using cardboard boxes. The sizes of the corridor and obstacle can be seen in Fig. 1(b). In order to explore the influence of obstacle size on pedestrian behaviour, the size of obstacle would be changed through adding the number of boxes that comprised the obstacle. As a result, five scenarios have been tested with the number of cardboard boxes comprising the obstacle being zero (without obstacle), one, two, three, and four boxes (i.e., $box=0, 1, 2, 3, 4$).

Pedestrians were asked to wear coloured knitted hats so that they could be easier recognized. During the experiments, pedestrians need to traverse the corridor one by one from the left exit to the right exit.

Besides, each pedestrian was asked to begin to walk only after his former pedestrian passed by the obstacle, and the heights of the boxes were set higher than human height. As a result, a pedestrian could not observe or copy the movement of other pedestrians and would take actions under his own willingness.

Each of the five sub-experiments that corresponded to the five scenarios would finish after all the 32 pedestrians traversed the corridor. Using the video data of the experiments, five sets of location data were obtained. Each set of data contained the real-time locations of 32 pedestrians, and the corresponding trajectories and velocities could be deduced accordingly.

3. Experimental results

When there is no obstacle in the corridor, a pedestrian can walk at his desired/free velocity. However, when there is an obstacle in the corridor as shown in Fig. 1 (a), a pedestrian has to evade the obstacle to traverse the corridor. In the evading process, he will decelerate in the horizontal direction and accelerate in the perpendicular direction, making it possible for us to investigate how the trajectory and velocity of a pedestrian would change during the evading process. In this study, we will analyse both the common and particular features of the evading process of single pedestrians.

3.1. Velocity variation

Through processing the video data, the location of each pedestrian at each frame can be obtained. In each data set (totally 5 sets of data), the velocity variation of 32 pedestrians could be calculated according to the location data. We assume that the location of a pedestrian at certain frame n is \vec{p}_n , the time at frame n is t_n , and the corresponding velocity v_n can be calculated according to the locations of pedestrians during a five frames interval (except for the first and last two frames of each sub-experiment) as below:

$$v_n = |\vec{p}_{n+2} - \vec{p}_{n-2}| / (t_{n+2} - t_{n-2}) \quad (1)$$

After calculating all the v_n at location \vec{p}_n of 32 pedestrians, we divided the x-axis by 0.1 meters into many x-sections, and the average value of the velocity points that fall into the same x-section is defined as the average velocity of this x-section. Therefore, the variation of average velocity with x-axis can be seen in Fig. 2. Please note that compared with normal coordinate system, the x axes of all the following figures have been reversed according to definition of x and y axis in Fig. 1 (b).

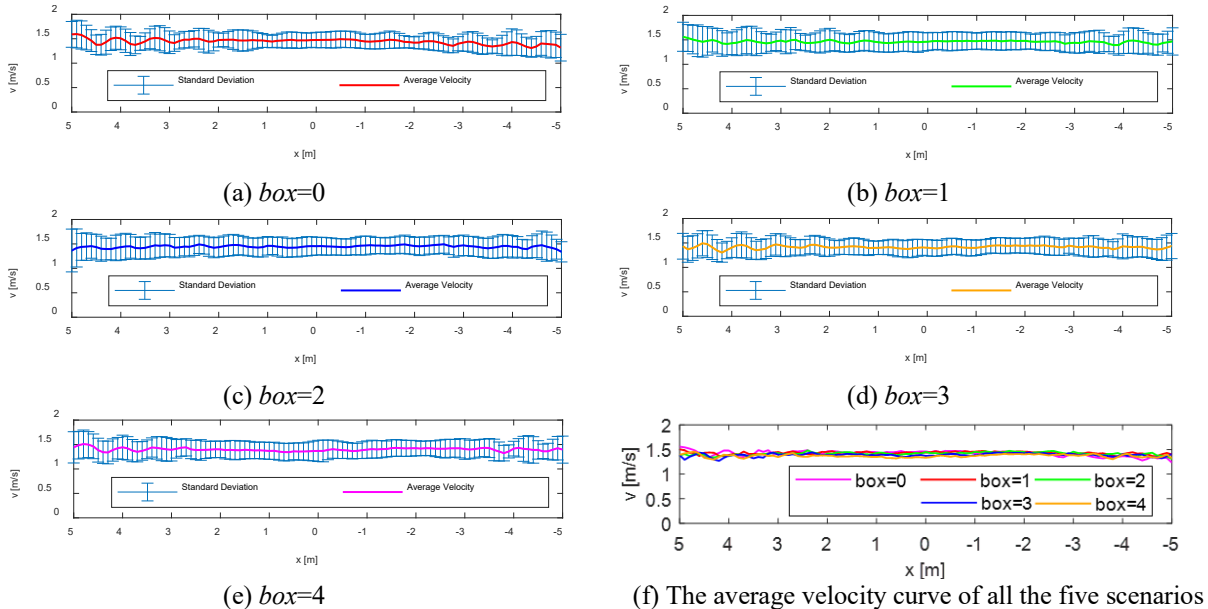


Fig. 2: Variation of average velocity and error bar at different positions along the corridor for five scenarios.

Through observing figures (a)-(e) in Fig. 2, it can be seen that the average velocity falls into 1.5 ± 0.2 m/s most of the time. Besides, the average velocity will not change a lot with the variation of x coordinate although pedestrians have to change the walking direction before and after evading the obstacle. Therefore, it can be deduced that pedestrians tend to keep walking at the desired velocity when evading an obstacle. Meanwhile, Fig. 3 (f) is plotted to compare the average velocity under the five scenarios. It can be seen that the average velocity under different obstacle sizes are nearly the same, which indicates that the existence or size of the obstacle will not affect the velocity of single pedestrian.

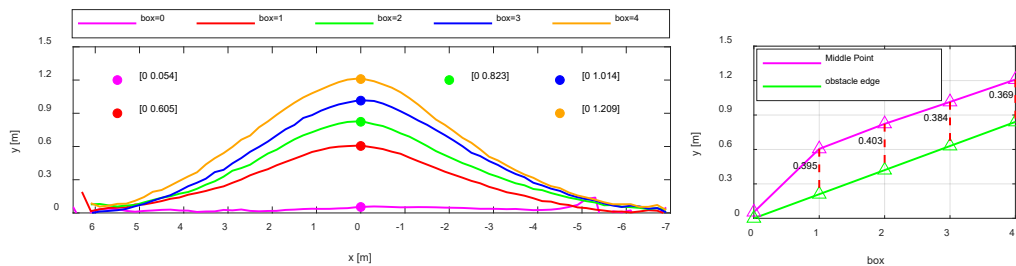
3.2. Variation of trajectory

Although a pedestrian tends to walk at constant velocity when encountering with an obstacle, he has to change his walking direction because he is physically unable to stride the obstacle. In this section, we analyse both the general and the particular features of pedestrian trajectories under different obstacle sizes.

Through observing the experiment process, we assume that pedestrians tend to follow the trajectory shown in Fig. 1 (a) when evading an obstacle. (This assumption will be proved by the linear curve fitting results afterwards.) When entering the corridor, a pedestrian tended to walk straight and then changed his walking direction to evade the obstacle. After passing by the obstacle, he would change his walking direction again until going back to the middle axis and then go straight to pass through the exit. The three critical locations that a pedestrian changed his walking direction are defined as Start Point (SP), Middle Point (MP) and End Point (EP) in this study.

The straight-walking process before SP and after EP is different from the common sense that pedestrians would choose the shortest path for least effort. We presume the psychological motivation behind the straight walking is our participants were not urgent to leave the corridor. As a result, they were probably more affected by the inertia to walk straight or just needed some time for reaction before evading the obstacle, and preferred a more comfortable walking direction before the exit.

To observe the general features of SP, MP and EP under each scenario, we first calculated the average trajectories of 32 pedestrians. The average trajectories and the MPs corresponding to the five average trajectories under five scenarios can be seen in Fig. 3 (a). Please note that the obstacle formed two bottlenecks with the walls in the corridor. Half of the participants passed by the obstacle from the upper bottleneck ($y > 0$) and the other half passed by from the lower one ($y < 0$). To obtain the average trajectory under each scenario, we reversed the trajectories of pedestrians who passed by the lower one by y-axis, and the y-coordinate of MP in Fig. 3 (a) is actually the average absolute values of all the MP coordinates of single pedestrians.



(a) average trajectories and MPs (b) y-coordinate of MP and obstacle edge
Fig. 3: The average trajectories of 32 pedestrians under five scenarios.

It can be seen from Fig. 3 (a) that the average trajectories of the five scenarios are smooth and symmetrical around the axis through $x = 0$, which is the location of the obstacle. Besides, the y-coordinate of the MP will increase with the rise of obstacle size. To illustrate the variation of MP more clearly and show the relation of MP with obstacle width, Fig. 3 (b) has been plotted.

Fig. 3 (b) shows that when there is an obstacle in the corridor ($box \geq 1$), the y-coordinate of MP will linearly increase with the rise of obstacle size. Meanwhile, the distance from the centroid of pedestrian to the obstacle edge that is perpendicular to the initial walking direction of pedestrians is also illustrated in Fig. 3 (b). Through comparison, we found that the distance from the MP to the edge of obstacle will always be

about 0.4 meters despite the variation of obstacle size. Analogously, Weidmann [14] already found that pedestrian tended to keep a distance from walls in the range of 0.2 – 0.45 meters depending on the type of wall. The results of our experiment are in well accordance with his findings.

On the other hand, although the location of MP can be achieved directly from the average trajectories, it is a little hard to get the coordinates of SP and EP directly. Therefore, we use a linear function in Eq. (2) to fit the average trajectories. An example for curve fitting is shown in Fig. 4, which illustrates the original and fitted trajectory of a certain pedestrian before the obstacle.

$$y = \begin{cases} a & (|x| \geq d) \\ bx + c & (|x| \leq d) \end{cases} \quad (2)$$

In Eq. (2), x and y respectively represent the x and y coordinate of the fitted curve, and a , b , c and d represent experimentally determined parameters. When $|x| \geq d$, the fitting equation actually equals to a . When $|x| \leq d$, the fitting equation actually equals to $bx + c$. The location point whose $|x|$ is closest to d among all the points before or after the obstacle is defined as SP ($x > 0$) or EP ($x < 0$) as shown in Fig. 4.

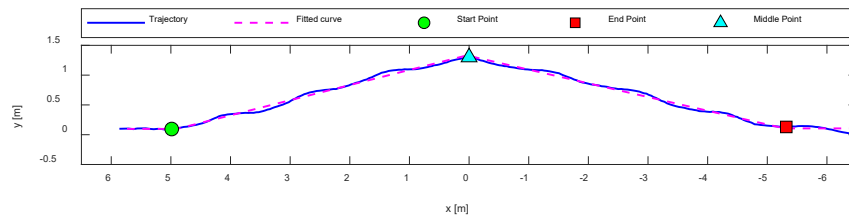


Fig. 4: Example for the curve fitting of trajectory, SP, MP and EP. ($box=4$, $R^2=0.9614$)

Based on Eq. (2), totally 128 trajectories (32 trajectories and four obstacle types) have been fitted. The R^2 of all the fitted curves are around 0.9810 ± 0.0144 , which can illustrate that the accuracy of this trajectory fitting method is high and the observed pedestrian evading pattern shown in Fig. 1 (a) is in accordance with real pedestrian movement. Therefore, the corresponding SPs and EPs can also be regarded as reliable. For better illustration, we define the distance from a SP to the obstacle as L_1 and the distance from an EP to the obstacle as L_2 . The distribution of L_1 and L_2 under the four obstacle sizes can be seen in Fig. 5.

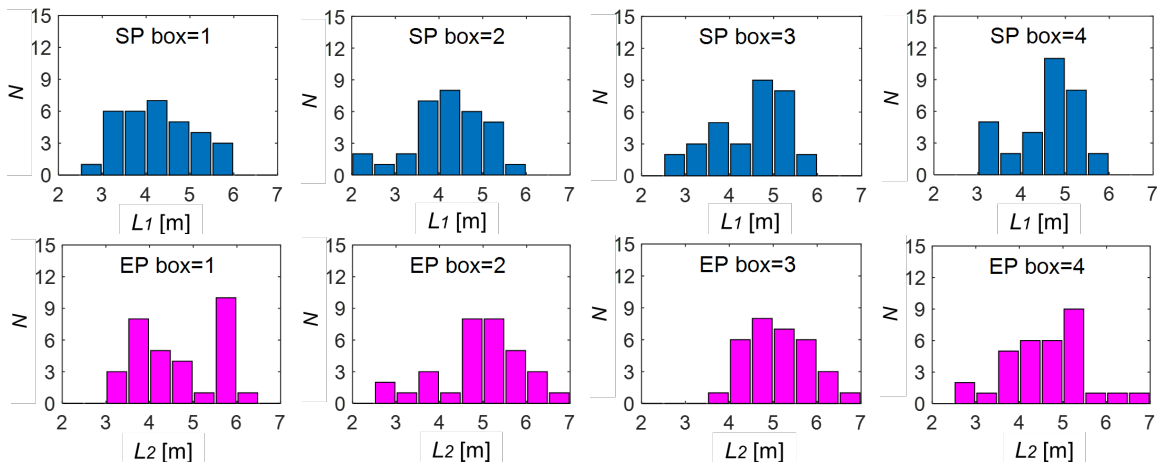


Fig. 5 Distribution of L_1 and L_2 of 32 pedestrians under four different obstacle sizes.

It can be seen from Fig. 5 that L_1 ranges from 2.0 to 6.0 meters and L_2 ranges from 2.5 to 7 meters. Besides, most L_1 are about 3.5 ~ 5.5 meters and most L_2 are about 4.0 ~ 6.0 meters. For further analysis, we calculate the average L_1 and L_2 under the four scenarios as shown in Table 1.

Table 1. Average L_1 and L_2 of 32 pedestrians under four obstacle sizes.

	$box=1$	$box=2$	$box=3$	$box=4$	Average
L_1 (m)	4.27	4.23	4.46	4.61	4.40
L_2 (m)	4.64	4.92	5.11	4.63	4.83

It can be seen from Table 1 that the average distance from SPs to the obstacle, i.e. average L_1 , is 4.40 meters. Besides, it can be seen that when box is small ($box=1$ and 2), L_1 will not change too much. Nevertheless, when the obstacle size is relatively large, L_1 will basically increase with the rise of box . We presume the reason is that when the obstacle size is small, people do not have to detour too much, and the variation of obstacle size has little influence on the evading behaviour of pedestrians. While when the obstacle size is large enough, pedestrians have to detour a longer distance, which might make them feel necessary to evade earlier either to walk more comfortably or evade with a shorter distance.

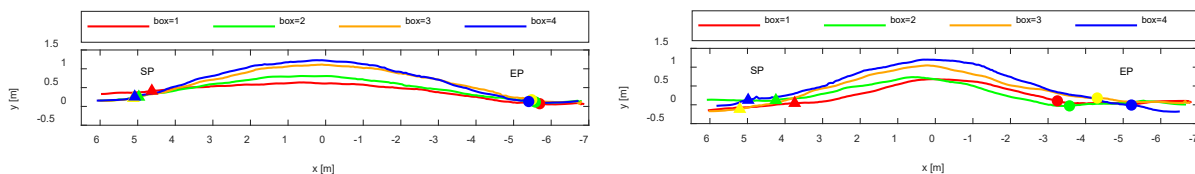
On the other hand, it can be seen from Table 1 that the average distance from EPs to the obstacle, i.e. L_2 , is 4.83 meters. Besides, L_2 will increase with the rise of obstacle size when box is 1, 2 and 3, which may be explained that the distance from the MP to the middle axis becomes larger with the rise of obstacle size, making pedestrians need to walk a longer distance in y direction and thus more or less increase the value of L_2 in x direction. However, when obstacle becomes too large ($box=4$), L_2 suddenly dropped about 0.5 meters, which shows that pedestrians prefer to return to the middle axis earlier when obstacle size is large enough, although the motivation of this movement is still not clear to us.

3.3 Classification of pedestrian behaviour

Despite that we have obtained some general features of the evading behaviour through calculating the average velocity and trajectories, we also found that different pedestrians show some particular features when encountering different-sized obstacles. Compared with the average trajectories in Fig. 3, trajectories of individual pedestrians are not always smooth or symmetric, which may be caused by the heterogeneity of pedestrians' perception and reaction to different walking environment.

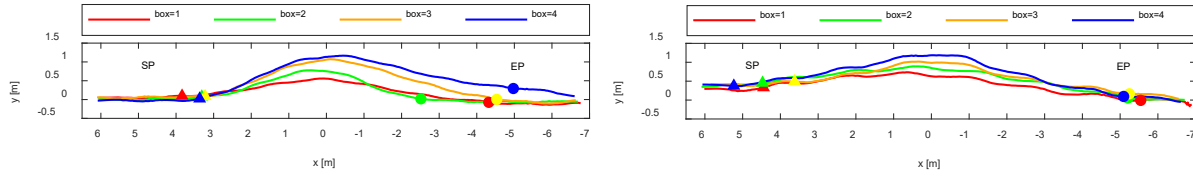
To each pedestrian, the location of SP and EP under each obstacle size can be obtained. However, the change of obstacle size has different influence on the change of SP and EP to different pedestrians. To better classify the heterogeneity of evading behaviour, we categorised pedestrians into four types based on the cluster degree of SPs and EPs under different obstacle sizes. With the variation of obstacle size, pedestrians belonging to Type 1 have similar SPs and EPs, pedestrians belonging to Type 2 have different SPs and EPs, pedestrians belonging to Type 3 have similar SPs but different EPs and pedestrians belonging to Type 4 have different SPs but similar EPs. Please note that we only focus on the x -locations of SPs and EPs while ignoring the y -locations. Besides, we assume that the SPs (or EPs) are similar when the mutual distances of x -locations are all smaller than gap meters. The value of gap is actually the critical distance that could distinguish the similarity of SPs and EPs.

Assuming $gap = 1.2$ m, we could obtain that among the 32 participants, the numbers of pedestrians belonging to Type 1, Type 2, Type 3 and Type 4 are 9 (28.1%), 12 (37.5%), 8 (25.0%) and 3 (9.4%) respectively. Fig. 6 shows the detailed trajectories, SPs and EPs of a certain pedestrian of each type.



(a) Type 1: with similar SPs and EPs

(b) Type 2: with different SPs and EPs



(c) Type 3: with similar SPs but different EPs (d) Type 4: with different SPs but similar EPs
Fig. 6: Illustration of the trajectories, SPs and EPs of pedestrians of four types with $gap = 1.2$ m.

Through reflecting on the whole moving process of pedestrians, we can assume that the evading behaviour begin when a pedestrian passes by the location of SP and terminate after passing the location of EP. Different pedestrians have different recognitions and reactions to the change of walking environment, making them make different decisions on where to start and finish the evading behaviour.

For pedestrians of Type 1 who tend to start and finish the evading behaviour at similar locations, we presume that they tend to follow certain stereotypes and the increase of obstacle size has little influence on their decision-making. For pedestrians of Type 2, they do not seem to follow certain evading pattern and the locations of their SPs and EPs are relatively dispersed. For pedestrians of Type 3, they tend to begin evading the obstacle at similar locations but finish the evading behaviour at different locations. For pedestrians of Type 4, pedestrians would begin to evade the obstacle at different locations but finish the evading behaviour at similar locations. However, the proportion of pedestrians of Type 4 is apparently smaller than that of the other three types. On the other hand, the value of gap also has influence on judging the similarity of SPs and EPs. Therefore, we depicted the variation of pedestrian number under each type with the value of gap increasing from zero to four meters, which can be seen in Fig. 7.

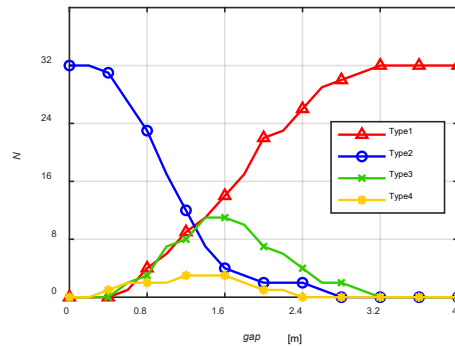


Fig. 7. Variation of pedestrian number of the four types with the increase of gap .

It can be seen from Fig. 7 that the value of gap will greatly affect the proportions of the four pedestrian types. When $gap = 0$ m, all the pedestrians belong to Type 2 because the SPs and EPs of a pedestrian cannot be exactly the same. When $gap = 3.2$ m, all the pedestrians belong to Type 1 because the maximum mutual distances of SPs and EPs of each pedestrian is not larger than 3.2 m. When $0 < gap < 3.2$ m, the critical distance to judge similarity becomes less rigorous than that when $gap = 0$ m and four types of pedestrians exist at the same time. Through comparison, we could see pedestrians of Type 1, Type 2 and Type 3 tend to have large pedestrian numbers. However, pedestrians belonging to Type 4 are always small, which means few people will have different SPs but similar EPs despite the value of gap .

4. Conclusion

This paper illustrates both the general and particular characteristics of the evading behaviour of single pedestrians in front of different-sized obstacle. Generally, a pedestrian tends to maintain his desired velocity and follow certain evading trajectories when encountering an obstacle. Besides, through calculating the average trajectory and accordingly obtain the average Middle Points, it can be seen that the distances from Middle Points to the edge of obstacle is always about 0.4 meters without being affected by the variation of

obstacle size. Moreover, the average value of the distances from SPs to the obstacle centroid (L_1) tends to show a rising trend with the increase of obstacle size. On the other hand, the average value of the distances from EPs to the obstacle centroid (L_2) also tends to increase with the rise of obstacle size but would suddenly decrease when obstacle size is large enough.

On the other hand, a heterogeneity in the evading behaviour has also been indicated. Through comparing the similarity of Start Points and End Points, pedestrians are classified into four types. Different types of pedestrians are supposed to have different perceptions and reactions to the obstacle. Although the critical mutual distance (*gap*) that defines the similarity of Start Points and End Points would affect the proportion of each pedestrian type, it seems that the number of pedestrians belonging to Type 4 is mostly the least despite the variation of critical mutual distance. Both the general and particular features are expected to contribute to developing more realistic evading rules in future related modelling and simulation.

Acknowledgements

This work was supported by JST-Mirai Program Grant Number JPMJMI17D4, Japan and JSPS KAKENHI Grant Number 15K17583. The first author is financially supported by Chinese Scholarship Council. In addition, the author would like to thank the team of Nishinari group for the assistance during the planning and conduction of the experiments in this paper.

References

- [1] V. Blue and J. Adler, "Modeling four-directional pedestrian flows," *Transportation Research Record*, vol. 1710, no. 1, pp. 20-27, 2000.
- [2] D. Helbing, I. Farkas and T. Vicsek, "Simulating dynamical features of escape panic," *Nature*, vol. 407, no. 6803, pp. 487-90, 2000.
- [3] P. Fiorini, "Motion planning in dynamic environments using velocity obstacles", *International Journal of Robotics Research*, vol. 17, no. 7, pp. 760-772, 1998.
- [4] C. Fulgenzi, A. Spalanzani, and C. Laugier, "Dynamic obstacle avoidance in uncertain environment combining PVOs and occupancy grid," *Proceeding of the IEEE International Conference on Robotics and Automation*, Rome, France, 2007, pp. 1610-1616.
- [5] Z. Zhou, Y. Liu, W. Wang, et al., "Multinomial logit model of pedestrian crossing behaviours at signalized intersections", *Discrete Dynamics in Nature and Society*, vol. 2013, pp. 1-8.
- [6] D. Yanagisawa, A. Kimura, A. Tomoeda, et al., "Introduction of frictional and turning function for pedestrian outflow with an obstacle", *Physical Review E*, vol. 80, no. 2, pp. 036110, 2009.
- [7] G. Frank and C. Dorso, "Room evacuation in the presence of an obstacle," *Physica A*, vol. 390, pp. 2135–2145, 2011.
- [8] M. Tang, H. Jia, B. Ran, et al., "Analysis of the pedestrian arching at bottleneck based on a bypassing behaviour model," *Physica A*, vol. 453, pp. 242–258, 2016.
- [9] S. Seer, N. Brändle and C. Ratti, "Kinects and human kinetics: A new approach for studying pedestrian behaviour," *Transportation Research Part C*, vol. 48, pp. 212-228, 2014.
- [10] X. Jia, H. Yue, X. Tian, et al., "Simulation of pedestrian flow with evading and surpassing behaviour in a walking passageway," *Simulation*, vol. 93, pp. 1013–1035, 2017.
- [11] M. Moussaïd, D. Helbing, S. Garnier, et al., "Experimental study of the behavioural mechanisms underlying self-organization in human crowds," *Proceedings of the Royal Society Biological Sciences*, vol. 276, no.1668, pp. 2755-2762, 2009.
- [12] W. Lv, W. Song, J. Ma, et al., "A two-dimensional optimal velocity model for unidirectional pedestrian flow based on pedestrian's visual hindrance field," *IEEE Transactions on Intelligent Transportation Systems*, vol. 14, no. 4, pp. 1753-1763, 2013.
- [13] M. Boltes and A. Seyfried, "Collecting pedestrian trajectories," *Neurocomputing*, vol. 100, pp. 127-133, 2013.
- [14] U. Weidmann, "Transporttechnik der fussgänger," *ETH Zürich*, vol. 90, 1992.